



This is a repository copy of *Probing human sperm metabolism using 13C-magnetic resonance spectroscopy*.

White Rose Research Online URL for this paper:
<http://eprints.whiterose.ac.uk/138606/>

Version: Accepted Version

Article:

Calvert, S.J., Reynolds, S. orcid.org/0000-0002-6463-8471, Paley, M.N. et al. (2 more authors) (2019) Probing human sperm metabolism using 13C-magnetic resonance spectroscopy. *Molecular Human Reproduction*, 25 (1). pp. 30-41. ISSN 1360-9947

<https://doi.org/10.1093/molehr/gay046>

Reuse

This article is distributed under the terms of the Creative Commons Attribution (CC BY) licence. This licence allows you to distribute, remix, tweak, and build upon the work, even commercially, as long as you credit the authors for the original work. More information and the full terms of the licence here:
<https://creativecommons.org/licenses/>

Takedown

If you consider content in White Rose Research Online to be in breach of UK law, please notify us by emailing eprints@whiterose.ac.uk including the URL of the record and the reason for the withdrawal request.



eprints@whiterose.ac.uk
<https://eprints.whiterose.ac.uk/>

1 **Probing human sperm metabolism**
2 **using ¹³C-magnetic resonance spectroscopy**

3
4 Running Title: ¹³C-MRS of human sperm metabolism

5
6 S. J. Calvert^{1*}, S. Reynolds^{2*}, M. N. Paley², S. J. Walters³, A. A. Pacey¹

7
8
9 ¹Academic Unit of Reproductive & Developmental Medicine, Department of
10 Oncology and Metabolism, University of Sheffield, Level 4, The Jessop Wing, Tree
11 Root Walk, Sheffield, S10 2SF, UK; ²Academic Unit of Radiology, Department of
12 Immunity, Infection and Cardiovascular Disease, University of Sheffield, Sheffield
13 S10 2JF; and ³School of Health Related Research, University of Sheffield, Regent
14 Court, 30 Regent Street, Sheffield, S1 4DA, UK.

15
16 * These authors contributed equally to the work.

17
18
19
20
21
22
23
24 © The Author 2018. Published by Oxford University Press on behalf of the European Society of Human
Reproduction and Embryology.

25 This is an Open Access article distributed under the terms of the Creative Commons Attribution License
(<http://creativecommons.org/licenses/by/4.0/>), which permits unrestricted reuse, distribution, and
reproduction in any medium, provided the original work is properly cited.

Abstract

26
27
28
29
30
31
32
33
34
35
36
37
38
39
40
41
42
43
44
45
46
47
48
49
50

STUDY QUESTION: Can ^{13}C -Magnetic Resonance Spectroscopy (MRS) of selected metabolites provide useful information about human sperm metabolism and how glycolysis or oxidative phosphorylation are used by different sperm populations?

SUMMARY ANSWER: Sperm populations, prepared by density gradient centrifugation (DGC) and incubated with either $^{13}\text{C}_\text{u}$ -glucose, $^{13}\text{C}_\text{u}$ -fructose or $^{13}\text{C}_\text{l}$ -pyruvate, showed consistent evidence of metabolism generating principally lactate and more intermittently bicarbonate, and significantly more lactate was produced from $^{13}\text{C}_\text{u}$ -glucose by vital or motile sperm recovered from the 40/80% interface compared to those from the pellet, which could not be accounted for by differences in the non-sperm cells present.

WHAT IS KNOWN ALREADY: Previous studies have focused on CO_2 or other specific metabolite production by human sperm and there remains considerable debate about whether glycolysis and/or oxidative phosphorylation is the more important pathway for ATP production in sperm.

STUDY DESIGN, SIZE, DURATION: Sperm populations were prepared by DGC and subjected to ^{13}C -MRS to answer the following questions. (i) Is it possible to detect human sperm metabolism of ^{13}C substrates implicated in energy generation? (ii) What are the kinetics of such reactions? (iii) Do different sperm populations (e.g. '80%' pellet sperm and '40%' interface sperm) utilise substrates in the same way? Semen samples from 97 men were used in these experiments; 52 were used in parallel for aims (i) and (ii) and 45 were used for aim (iii).

51

52 **PARTICIPANTS/MATERIALS, SETTING, METHODS:** Sperm populations were
53 prepared from ejaculates of healthy men using a Percoll/Phosphate Buffered Saline
54 (PBS) DGC and then incubated with a range of ^{13}C -labelled substrates ($^{13}\text{C}_\text{U}$ -
55 glucose, $^{13}\text{C}_\text{U}$ -fructose, $^{13}\text{C}_1$ -pyruvate, $^{13}\text{C}_1$ -butyrate, $^{13}\text{C}_3$ -lactate, $^{13}\text{C}_{2,4}$ -D-3-
56 hydroxybutyrate, $^{13}\text{C}_5$ -L-glutamate, $^{13}\text{C}_{1,2}$ -glycine or $^{13}\text{C}_\text{U}$ -galactose) along with
57 penicillin/streptomycin antibiotic at 37°C for 4 hours, 24 hours or over 48 hours for an
58 estimated rate constant. Sperm concentration, vitality and motility were measured
59 and, for a subset of experiments, non-sperm cell concentration was determined. A
60 9.4T magnetic resonance spectrometer was used to acquire 1D ^{13}C , inverse gated
61 ^1H decoupled, MRS spectra. Spectrum processing was carried out using
62 spectrometer software and Matlab scripts to determine peak integrals for each
63 spectrum.

64

65 **MAIN RESULTS AND THE ROLE OF CHANCE:** $^{13}\text{C}_\text{U}$ -glucose, $^{13}\text{C}_\text{U}$ -fructose and
66 $^{13}\text{C}_1$ -pyruvate were consistently converted into lactate and, to a lesser extent,
67 bicarbonate. There was a significant correlation between sperm concentration and
68 lactate peak size for $^{13}\text{C}_\text{U}$ -glucose and $^{13}\text{C}_\text{U}$ -fructose, which was not observed for
69 $^{13}\text{C}_1$ -pyruvate. The lactate peak did not correlate with the non-sperm cell
70 concentration up to $6.9 \times 10^6/\text{ml}$. The concentration of $^{13}\text{C}_\text{U}$ -glucose, $^{13}\text{C}_\text{U}$ -fructose or
71 $^{13}\text{C}_1$ -pyruvate (1.8, 3.6, 7.2 or 14.4 mM) had no influence on the size of the observed
72 lactate peak over a 4 hour incubation. The rate of conversion of $^{13}\text{C}_1$ -pyruvate to
73 lactate was approximately three times faster than for $^{13}\text{C}_\text{U}$ -glucose or $^{13}\text{C}_\text{U}$ -fructose
74 which were not significantly different from each other. After incubating for 4 hours,
75 the utilisation of $^{13}\text{C}_\text{U}$ -glucose, $^{13}\text{C}_\text{U}$ -fructose or $^{13}\text{C}_1$ -pyruvate by sperm from the

76 '40%' interface of the DGC was no different from those from the pellet when
77 normalised to total sperm concentration. However, after normalising by either the
78 vital or motile sperm concentration, there was a significant increase in conversion of
79 $^{13}\text{C}_u$ -glucose to lactate by '40%' interface sperm compared to pellet sperm (Vital =
80 $3.3 \pm 0.30 \times 10^6$ vs $2.0 \pm 0.21 \times 10^6$; $p = 0.0049$; Motile = $7.0 \pm 0.75 \times 10^6$ vs 4.8 ± 0.13
81 $\times 10^6$; $p = 0.0032$. Mann-Whitney test $p < 0.0055$ taken as statistically significant). No
82 significant differences were observed for $^{13}\text{C}_u$ -fructose or $^{13}\text{C}_1$ -pyruvate.

83

84 **LARGE SCALE DATA:** Not applicable.

85

86 **LIMITATIONS, REASONS FOR CAUTION:** Only ^{13}C labelled metabolites that
87 accumulate to a sufficiently high concentration can be observed by ^{13}C MRS. For this
88 reason, intermediary molecules in the metabolic chain are difficult to observe without
89 trapping the molecule at a particular step using inhibitors. Non-sperm cell
90 concentration was typical of the general population and no link was found between
91 these cells and the magnitude of the ^{13}C -lactate peak. However, it is possible that
92 higher concentrations than the maximum observed ($6.9 \times 10^6/\text{ml}$) may contribute to
93 exogenous substrate metabolism in other experiments.

94

95 **WIDER IMPLICATIONS OF THE FINDINGS:** ^{13}C -MRS can provide information on
96 the underlying metabolism of multiple pathways in live sperm. Dysfunction in sperm
97 metabolism, as a result of either impaired enzymes or lack of metabolisable
98 substrate, could be detected in sperm by a non-destructive assay, potentially offering
99 new treatment options to improve overall sperm quality and outcomes for
100 reproduction.

101

102

103 **STUDY FUNDING AND COMPETING INTEREST(S):** This work was supported by
104 the Medical Research Council Grant MR/M010473/1. The authors declare no
105 conflicts of interest.

106

107 **KEYWORDS:** magnetic resonance spectroscopy, metabolism, glycolysis, Krebs
108 cycle, human sperm

109

110 **Introduction**

111 Poor sperm quality significantly contributes to cases of infertility within couples
112 (Pacey, 2009), yet many basic aspects of sperm physiology remain unknown (Barratt
113 *et al.*, 2018). One important and unanswered question is how human sperm
114 generate the ATP (adenosine triphosphate) necessary to sustain motility and
115 undergo the metabolically demanding processes of capacitation and hyperactivation
116 (Suarez and Pacey, 2006). Furthermore, such information may be useful both to help
117 understand the molecular causes of poor sperm motility (e.g. asthenozoospermia)
118 and to provide insights into targets for novel agents to enhance sperm motility.

119

120 After more than 50 years of research, it is now clear that human sperm can produce
121 ATP through the metabolic processes of glycolysis and/or oxidative phosphorylation
122 (du Plessis *et al.*, 2015). This has been examined using a variety of experimental
123 approaches over the years, including: (i) the measurement of oxygen consumption of
124 washed sperm either in the presence (Ford and Harrison, 1981) or absence
125 (Peterson and Freund, 1970) of metabolic inhibitors; (ii) incubation with ¹⁴C
126 radiolabelled substrates (Ford and Harrison, 1981, Murdoch and White, 1968); (iii)
127 the measurement of ADP and ATP in semen samples with different phenotypes
128 (Vigue *et al.*, 1992); and (iv) the use of proteomics to identify new metabolic
129 enzymes and pathways (Amaral *et al.*, 2014). However, there remains considerable
130 debate about whether glycolysis and/or oxidative phosphorylation is more important
131 for the various aspects of human sperm function during their post-ejaculatory life (du
132 Plessis *et al.*, 2015, Ruiz-Pesini *et al.*, 2007).

133

134 In a recent paper, we used ^1H Magnetic Resonance Spectroscopy (MRS) to examine
135 the endogenous metabolome of live human sperm isolated from semen using
136 40/80% Density Gradient Centrifugation (DGC) (Reynolds *et al.*, 2017a). This
137 showed that several metabolite peaks, including those associated with lactate, could
138 be used to discriminate sperm recovered from the pellet ('80%' sperm) from those
139 recovered from the '40%' interface. As '80%' sperm typically have better motility, this
140 suggested that there may be important metabolic differences between these two
141 sperm populations with respect to their utilisation of the pathways of glycolysis and
142 oxidative phosphorylation.

143

144 ^{13}C -MRS has been used to examine metabolic pathways in other cell types
145 (Buescher *et al.*, 2015) including metabolic regulation in cancer cells (Shestov *et al.*,
146 2016). Using ^{13}C labelled substrates provides three advantages. Firstly, they are
147 metabolised the same as those found within human physiology and their ^{13}C -MRS
148 spectra are greatly simplified compared to ^1H MRS, displaying known peaks for the
149 source substrate and those peaks having arisen from cellular metabolism. Secondly,
150 particular metabolic pathways can be identified through strategic placement of the
151 ^{13}C label (Buescher *et al.*, 2015). Alternative or multiple pathways can be assayed
152 through varying ^{13}C labelling patterns, even if the end product is the same (Bruntz *et*
153 *al.*, 2017). Finally, the cells under study remain viable throughout the experiment and
154 therefore can be measured at multiple time points (Reynolds *et al.*, 2017b).

155

156 As many aspects of sperm metabolism remain unknown and ^{13}C -MRS can provide
157 insights into metabolism in live cells, we reasoned that this combination would be
158 able to further elucidate the metabolic pathways used by live human sperm. In this

159 paper, we use ^{13}C -MRS to investigate three questions. (i) Is it possible to detect
160 human sperm metabolism of ^{13}C substrates implicated in energy generation? (ii)
161 What are the kinetics of such reactions? (iii) Do different sperm populations (e.g.
162 '80%' and '40%' sperm) utilise substrates in the same way?

163

164 **Materials and methods**

165 Semen donation and analysis

166 Semen samples were obtained from men attending the Andrology Laboratory
167 (Jessop Wing, Sheffield, UK) for semen analysis (approved by the North of Scotland
168 Research Ethics Committee (16/NS/0009) on 17/02/16). Informed consent was
169 obtained from each man to use their ejaculates in this project and semen samples
170 were produced after at least two days of sexual abstinence. Each ejaculate was
171 collected into a sterile plastic container (Sarstedt, Leicester, UK) and examined
172 according to World Health Organisation (2010) methods within one hour of
173 production. Samples selected for experiments contained at least a total of 25×10^6
174 sperm and 40% progressively motile sperm, as these contain sufficient sperm of
175 normal motility to complete sample preparation.

176

177 Sperm preparation techniques

178 Sperm were isolated from seminal plasma using DGC based on the methods
179 outlined in Reynolds *et al.* (2017a) and summarised in Figure 1. Briefly, this involved
180 placing approximately 1 ml of liquefied semen on either 40% (v/v) (Process A for
181 aims i and ii) or layered 40% and 80% (v/v) (Process B for aims iii) Percoll/PBS
182 solution (Percoll, GE Healthcare Life Sciences, Little Chalfont, UK) in a 13 ml
183 polypropylene tube with ventilation cap (Sarstedt, Leicester, UK). These were then

184 centrifuged for 20 minutes at 300 *g* to produce an unfractionated pellet (Process A)
185 or a population of sperm trapped at the 40-80% interface (termed '40%' sperm) and
186 those found at the bottom of the tube (termed '80%' sperm) (Process B). In both
187 cases, these sperm were re-suspended in PBS to at least three times their
188 recovered volume before being centrifuged again for 10 minutes at 500 *g*. At each
189 stage, the supernatant was removed, and the sperm was suspended in fresh PBS to
190 a minimum volume of 600 μ l.

191

192 Baseline measurements

193 From each prepared sample, a 2.5 μ l aliquot was placed in a 10 μ m depth Leja
194 chamber (Leja Products, Nieuw Vennep, the Netherlands) which was then placed on
195 a heated plate at 37°C for 5 minutes before measuring concentration and motility
196 using Sperm Class Analyzer, version 6 (Microptic SL, Barcelona, Spain) attached to
197 a Microtec LM-2 Microscope (Mazurek Optical Services Ltd, Southam, UK) via a
198 Basler acA1300-200uc camera (Basler AG, Ahrensburg, Germany). Since PBS does
199 not contain any metabolites, sperm suspended in it generally swim poorly and so this
200 process was repeated with a 20 μ l aliquot of prepared sperm diluted 1 in 2 in
201 PureSperm Wash (Nidacon, Gothenburg, Sweden) to assess the ability of the
202 prepared sperm to swim when placed in a conventional medium. In addition, sperm
203 vitality of each prepared sample was assessed using the LIVE/DEAD™ sperm
204 viability kit (Fisher Scientific, Loughborough, UK), counting two replicates of at least
205 200 sperm as either alive (green) or dead (red) in order to establish the percentage
206 of viable sperm.

207

208 Sperm incubation with ¹³C substrates

209 In order to identify which ^{13}C labelled substrates could be metabolised by sperm (aim
210 i), 400 μl of unfractionated sperm (prepared by Process A in Figure 1) was added to
211 a 5 ml snap cap polystyrene round-bottom tube (Corning Falcon, Fisher Scientific)
212 along with 15 μl antibiotics (10000 units/ml penicillin and 10 mg/ml streptomycin
213 diluted to 1/3 with PBS so that in tube concentrations were 90 units/ml penicillin and
214 90 $\mu\text{g/ml}$ streptomycin, Sigma Aldrich) and 40 μl of 100 mM ^{13}C labelled substrate (to
215 give a final concentration of 8.8 mM). The substrates (obtained from either Sigma
216 Aldrich or Cambridge Isotopes Laboratories, Tewksbury, MA, USA) tested were:
217 $^{13}\text{C}_\text{u}$ -glucose, $^{13}\text{C}_\text{u}$ -fructose, $^{13}\text{C}_1$ -pyruvate, $^{13}\text{C}_1$ -butyrate, $^{13}\text{C}_3$ -lactate, $^{13}\text{C}_{2,4}$ -D-3-
218 hydroxybutyrate, $^{13}\text{C}_5$ -L-glutamate (prepared from glutamic acid), $^{13}\text{C}_{1,2}$ -glycine and
219 $^{13}\text{C}_\text{u}$ -galactose. Each substrate was incubated for 24 hours at 37°C with 8 samples of
220 prepared sperm from individual men and where possible more than one substrate
221 incubation was performed in parallel (in these cases the sperm were always shown
222 to metabolise at least one substrate). After each incubation the sample was frozen at
223 -80°C until MRS analysis (see below).

224
225 For each substrate found in aim (i) to be consistently metabolised by washed sperm,
226 the rate constant was estimated for sperm from 9 ejaculates to determine substrate
227 kinetics (aim ii). Briefly, from each ejaculate, a 380 μl aliquot of unfractionated sperm
228 (Figure 1, Process A) was placed in a 5 mm MRS tube along with 40 μl of 100mM
229 ^{13}C labelled substrate, 10 μl ^{13}C -urea (concentration and frequency reference), 20 μl
230 D_2O and 12 μl of antibiotics (as above). The tube was inserted into the MRS scanner
231 which had been preheated to 37°C and a series of sequential ^{13}C -spectra were then
232 acquired approximately every 3 hours (see below for details) until the change in the
233 magnitude of the MRS peaks began to plateau, typically over a 18- 48 hour period.

234

235 To assess the effect of substrate concentration on sperm metabolism (aim ii),
236 incubations were performed with unfractionated sperm (Figure 1, Process A) and ^{13}C
237 labelled substrates consistently metabolised by sperm, identified in aim (i), (n=3).
238 From each ejaculate, 460 μl of unfractionated sperm, 15 μl of antibiotics and 80 μl of
239 ^{13}C labelled substrate diluted to a final concentration of 0, 1.8, 3.6, 7.2 or 14.4 mM
240 was incubated for 4 hours at 37°C in a 5 ml snap cap polystyrene round-bottom tube
241 (Corning Falcon, Fisher Scientific). At the end of the incubation, each sample was
242 frozen at -80°C until MRS analysis.

243

244 Metabolism differences between '40%' and '80%' sperm (aim iii), were examined by
245 incubating 500 μl of each (prepared from individual samples using Process B shown
246 in Figure 1) with 15 μl of antibiotics and 40 μl of the 100 mM ^{13}C labelled substrates,
247 identified in aim (i) and confirmed in aim (ii), for 4 hours at 37°C (n=15). Samples
248 were then frozen at -80°C until MRS analysis.

249

250 To assess the potential impact of any non-sperm cells present in the sperm fractions
251 obtained for aim (iii), the concentration of non-sperm cells was determined according
252 to the method outlined in WHO (2010). Briefly, 10 μl from each sperm preparation
253 was smeared onto two polysine slides (Thermo Scientific, Saarbrücken Germany),
254 and after air-drying stained with Diff-Kwik kit (Thermo Scientific) and imaged on a
255 Microtec LM-2 microscope at 40 x magnification. At least 400 sperm were counted
256 along with any non-sperm cells observed in these fields of view; sperm heads
257 without tails were excluded from the analysis. The concentration of non-sperm cells
258 was determined using the formula in WHO (2010).

259

260 Magnetic Resonance Spectroscopy (MRS)

261 All samples were scanned using a 9.4 T Bruker Avance III MRS spectrometer
262 (Bruker BioSpin GmbH, Karlsruhe, Germany), with a 5 mm broadband observe
263 probe operating at either room temperature ($21^{\circ}\text{C} \pm 0.5$) for the frozen-thawed
264 samples or at ($37^{\circ}\text{C} \pm 0.5$) for the experiments carried out for the rate constant
265 experiments in aim (ii). Samples that were frozen at -80°C were thawed and 380 μl
266 was placed in a 5 mm MRS tube (Norell, Morganton, NC, USA) with 20 μl D_2O
267 (Sigma Aldrich) and 10 μl of 200 mM ^{13}C -urea (chemical shift and concentration
268 reference, Sigma Aldrich) for MRS analysis. Spectra were acquired using a $^{13}\text{C}\{^1\text{H}\}$
269 inverse-gated pulse sequence (Spectral Width = 239 ppm, Number of acquisitions =
270 4096, Acquisition Time = 0.5 s, Delay Time = 2 s, Time domain points = 24036, flip
271 angle = 16°). Each acquired spectrum was apodised with a 5 Hz exponential line
272 broadening function, phase and baseline corrected using Bruker Topspin v2.1
273 software and referenced to the urea signal at a frequency offset $\delta = 165.5$ ppm.

274

275 Data analysis

276 For aim (i), all ^{13}C -MRS spectra were first inspected visually by an expert in MRS
277 (SR) for evidence of substrate metabolism, which could be identified by the
278 appearance of new metabolite peaks and a visual reduction in the peak height of the
279 ^{13}C labelled substrate added. Identification of unknown peaks present in the spectra
280 was assisted by reference to relevant metabolic pathways known to utilise the
281 substrate and chemical shift values obtained from the human metabolome database
282 version 4.0 (Wishart *et al.*, 2018).

283

284 All ^{13}C -spectra peaks were integrated using the 'trapz' function in a custom Matlab
285 script (R2017b, Mathworks, Natick, MA, USA) and predefined chemical shift integral
286 ranges as appropriate for the substrate molecule (185.8-184.8 ppm, $^{13}\text{C}_1$ -lactate;
287 173.5-172.5 ppm, $^{13}\text{C}_1$ -pyruvate; 166.0-165.0 ppm, ^{13}C -urea; 163.5-162.7 ppm, ^{13}C -
288 bicarbonate; 127.9-127.3 ppm, $^{13}\text{CO}_2$; 99.2-98.2 ppm, $^{13}\text{C}_u$ -glucose; 102-99.6 ppm,
289 $^{13}\text{C}_u$ -fructose; 71.5-70.5 ppm, $^{13}\text{C}_2$ -lactate; 23.4-22.4 ppm, $^{13}\text{C}_3$ -lactate). The
290 integrals for peaks assigned to bicarbonate and carbon dioxide were summed to
291 account for the biological equilibrium in which these molecules exist.

292

293 To examine rates of metabolism in aim (ii), each set of sequentially acquired ^{13}C -
294 spectra obtained from a single experiment were imported into Matlab and collated
295 into sets of peak integral time courses obtained from each spectrum. Integrals
296 versus time for each peak were plotted and fitted to either a mono-exponential
297 growth (lactate and bicarbonate/ CO_2 peaks) or mono-exponential decay (glucose,
298 fructose and pyruvate). Only fits to the data that had a Pearson correlation of $r > 0.5$
299 and a $p < 0.01$ were retained in order to avoid misestimation of rate values due to
300 poor signal to noise (principally arising from the bicarbonate/ CO_2 integrals). The
301 mean \pm standard error (S.E.) was determined for each peak from each source
302 substrate. Differences between metabolic rates were tested using a one-way
303 ANOVA with Bonferroni post-hoc multi-comparison test $p < 0.05$ taken as significant.

304

305 The effect of concentration of supplied substrate on sperm metabolism (aim ii) was
306 analyzed by measuring lactate integrals for the integral from the $^{13}\text{C}_1$ position
307 (normalised by total sperm concentration) across the concentration ranges and
308 comparing them using a Kruskal-Wallis test with $p < 0.05$ taken as significant.

309

310 The correlation between $^{13}\text{C}_\text{u}$ -glucose, $^{13}\text{C}_\text{u}$ -fructose or $^{13}\text{C}_1$ -pyruvate derived lactate
311 integrals and total sperm concentration was determined by Pearson linear regression
312 using GraphPad Prism (version 7.03, La Jolla, USA). The value of r^2 and significance
313 of the correlation are reported for the fit. A similar regression fit was also performed
314 between lactate integral and non-sperm cell concentration.

315

316 In the comparison of metabolism by '40%' and '80%' sperm (aim iii), the spectra from
317 co-incubation of '40%' or '80%' sperm with ^{13}C substrates were initially phase- and
318 baseline-corrected and referenced to the urea peak as above. Custom MatLab code
319 was then used to integrate the lactate peak between 185.8-184.8ppm and the
320 bicarbonate peak between 163.5-162.7ppm. These integrals were then normalised
321 according to: (a) sperm concentration; (b) concentration of vital sperm; and (c)
322 concentration of motile sperm (where the motility was determined for sperm in
323 PureSperm wash at time zero – see above). In all of these normalisations, the
324 concentration of sperm in PBS was used. Normalised substrate integrals were
325 compared between '40%' and '80%' sperm by Mann-Whitney with $p < 0.0055$ taken
326 as significant (0.05/9 as 9 comparisons were done).

327

328 **Results**

329 Semen samples from 97 men, recruited as part of a larger study, were used in these
330 experiments; 52 were used in parallel for aims (i) and (ii) and 45 were used for aim
331 (iii).

332

333 Aim (i): Assessment of metabolically active substrates

334 The ability of ^{13}C -MRS to detect human sperm metabolism was tested eight times,
335 for each of the 9 substrates associated with energy generation, over a 24 hour
336 incubation period. This showed that the metabolism of ^{13}C substrates directly
337 involved in the glycolytic pathway, glucose, fructose and pyruvate, were easily
338 detected through conversion to lactate (Table 1). Whilst conversion to lactate was
339 always observed for these molecules, bicarbonate/ CO_2 was not (however,
340 bicarbonate/ CO_2 peaks were observed in a subset of experiments from aim (ii)
341 (Figure 2) and aim (iii), see below). Incubation with $^{13}\text{C}_3$ -lactate showed shuttling to
342 pyruvate in most samples (7 of 8) and this was often accompanied by production of
343 peak associated with an acetyl methyl group (6 of 8), which could be from
344 dissociated acetyl-coA. Two of these eight experiments also showed $^{13}\text{C}_3$ -lactate
345 metabolism to bicarbonate/ CO_2 . Of the other ^{13}C substrates, small quantities of
346 acetoacetate were metabolised from $^{13}\text{C}_{2,4}$ -D-3-hydroxybutyrate, but further
347 metabolism (including entry into the Krebs cycle) was not detected. There was no
348 evidence of regular metabolism of $^{13}\text{C}_1$ -butyrate, $^{13}\text{C}_5$ -glutamate and $^{13}\text{C}_{1,2}$ -glycine by
349 sperm, however, there was occasional production of bicarbonate by these substrates
350 (Table 1). Finally, in these 8 samples, incubation with $^{13}\text{C}_u$ -galactose analysis by ^{13}C -
351 MRS showed only the original $^{13}\text{C}_u$ -galactose peaks. Example ^{13}C -spectra from other
352 24h incubations are shown in Supplementary Figures S1-S6.

353

354 Aim (ii): Substrate kinetics of human sperm

355 In order to establish the appropriate conditions for sperm/substrate incubations in
356 MRS experiments $^{13}\text{C}_u$ -glucose, $^{13}\text{C}_u$ -fructose, $^{13}\text{C}_1$ -pyruvate and $^{13}\text{C}_3$ -lactate were
357 selected for further analysis to examine their kinetics and optimum concentration for
358 metabolism. Sperm from 31 ejaculates were used to determine rate constants: $n = 9$

359 each for $^{13}\text{C}_u$ -glucose, $^{13}\text{C}_u$ -fructose, and $^{13}\text{C}_1$ -pyruvate; $n = 4$ for $^{13}\text{C}_3$ -lactate.
360 Repeated sequential acquisition of spectra ($n = 9$ for $^{13}\text{C}_u$ -glucose, $^{13}\text{C}_u$ -fructose,
361 $^{13}\text{C}_1$ -pyruvate; $n = 2$ for $^{13}\text{C}_3$ -lactate) showed mono-exponential growth and decay in
362 product and source substrate respectively (see supplementary Figures S7-S9). The
363 rates of metabolite production and substrate consumption can be seen in Table 2,
364 excluding $^{13}\text{C}_3$ -lactate which did not provide reliable measures of metabolism.

365

366 Universally isotopically labelled $^{13}\text{C}_u$ -glucose and $^{13}\text{C}_u$ -fructose will label all three
367 carbons of lactate whereas $^{13}\text{C}_1$ -pyruvate will only be converted to $^{13}\text{C}_1$ -lactate. An
368 ANOVA test with Bonferroni post-hoc test showed that the choice of lactate peak (1,
369 2 or 3) had no significant effect on the estimated rate constant derived from $^{13}\text{C}_u$ -
370 glucose ($p = 0.99$) or $^{13}\text{C}_u$ -fructose ($p = 0.69$). Given that a fructose MRS peak
371 obscures the C2 labelled position of lactate and the pyruvate labels only C1,
372 therefore, only the $^{13}\text{C}_1$ peak of lactate was used for subsequent analysis. This
373 showed that there was no significant difference (ANOVA with Bonferroni post-hoc
374 test) in the rate of $^{13}\text{C}_u$ -glucose ($1.7 \pm 0.4 \times 10^{-5} \text{ s}^{-1}$) or $^{13}\text{C}_u$ -fructose ($1.4 \pm 0.2 \times 10^{-5}$
375 s^{-1}) conversion to lactate. However, the single enzymatic step of $^{13}\text{C}_1$ -pyruvate to
376 lactate ($5.0 \pm 0.8 \times 10^{-5} \text{ s}^{-1}$) was approximately three times faster than that of $^{13}\text{C}_u$ -
377 glucose and $^{13}\text{C}_u$ -fructose ($p = 0.0011$ and $p = 0.00042$, respectively). Visually
378 inspecting the rate data showed that typically $^{13}\text{C}_1$ -pyruvate incubations reached
379 over half the maximum lactate production by the second time point (an average of
380 4.5 hours into the experiment), whereas from $^{13}\text{C}_u$ -glucose and $^{13}\text{C}_u$ -fructose, over
381 half the maximum lactate production was often reached at the sixth time point (an
382 average of 19.5 hours into the incubation).

383

384 In contrast to 24 h incubations (aim i), bicarbonate was produced during some rate
385 experiments (aim ii). It appeared more frequently from $^{13}\text{C}_1$ -pyruvate (6 of 8) than
386 $^{13}\text{C}_6$ -glucose (3 of 8), although the rate constants for these were not significantly
387 different. This was probably due to the smaller peak intensity causing large standard
388 error in the rate constant (see Table 2). $^{13}\text{C}_6$ -fructose did not produce bicarbonate
389 under these conditions. Sequential spectra were also acquired where $^{13}\text{C}_3$ -lactate
390 was the source substrate, however, in these experiments no consistent build-up of
391 pyruvate or bicarbonate/ CO_2 was observed (n=4), most likely due to the low signal to
392 noise of the pyruvate peak that had been observed for $^{13}\text{C}_3$ -lactate from aim (i). A
393 long incubation allows time for MRS peaks to increase leading to a reduction in
394 integration errors due to signal noise. However, sperm quality also degrades with
395 time, therefore, 4 hours was chosen for subsequent experiments.

396

397 The optimum metabolite concentrations were assessed during a 4 hour incubation
398 for the principal metabolic substrates of $^{13}\text{C}_6$ -glucose, $^{13}\text{C}_6$ -fructose and $^{13}\text{C}_1$ -
399 pyruvate (three washed sperm samples per substrate). Overall, the amount of lactate
400 produced by sperm (normalised to total sperm concentration) was not significantly
401 influenced by the supplied substrate concentration (1.8 - 14.4 mM) (see Figure 3 and
402 supplementary Figure S10). However, after 4 hours of incubation the remaining
403 substrate peaks for the lowest concentration, 1.8 mM, were almost absent from the
404 MRS spectrum. Consequently, to ensure substrate metabolism was not limited by its
405 availability and to allow for higher sperm concentration than used here in subsequent
406 experiments, a concentration of 7.2 mM was selected for the experiments in aim (iii).

407

408 Aim (iii): Substrate Metabolism by '40%' and '80%' sperm

409 Sperm metabolism was assessed using sperm from 45 individual ejaculates that had
410 been separated by DGC (Process B in Figure 1). This method yields two sperm
411 populations (termed '40%' and '80%' sperm in Reynolds *et al.*, 2017a) with
412 significant differences in both motility and vitality (see Table 3). The percentage
413 sperm motility were not similar to the viability (i.e. sperm motility was not entirely due
414 to a lack of viable sperm) and, importantly for our study, there was no significant
415 difference in sperm concentration between the '40%' and '80%' groups.

416

417 The '40%' and '80%' sperm samples also contained small numbers of other cell
418 types (e.g. leukocyte, germ and epithelial cells) that may have been metabolically
419 active. Therefore, it was important to determine their prevalence in the sperm
420 preparations assessed in aim (iii). Briefly, there were more non-sperm cells in the
421 '40%' compared to the '80%' sperm population (median: 1.1, range: 0.1 – 6.9 vs.
422 median: 0.4, range: 0.0 – 4.5 x 10⁶/ml, $p < 0.0001$, respectively). Both fractions
423 showed a correlation between the concentration of non-sperm cells and sperm
424 concentration but the r^2 was higher for the '40%' sperm fraction ($p = 0.0018$, $r^2 =$
425 0.21), than the '80%' fraction ($p = 0.046$, $r^2 = 0.09$), see supplementary Figure S11.

426

427 The '40%' and '80%' sperm were separated into cohorts incubated with different
428 substrates ($n = 15$ samples per sperm population) with sperm concentration, vitality
429 and motility measured at the start of incubation (Table 4). A Kruskal-Wallis test with
430 a Dunn's multiple comparison correction showed that none of these parameters were
431 significantly different for the '80%' or the '40%' sperm for any substrate.

432

433 Lactate peaks in the ^{13}C -MRS spectra were plotted against total sperm concentration
434 to determine whether the observed lactate arose from sperm metabolism. When
435 sperm were incubated with either $^{13}\text{C}_\text{u}$ -glucose or $^{13}\text{C}_\text{u}$ -fructose, there was a
436 significant strong linear correlation with total sperm concentration (see Figures 4a
437 and 4b). However, the lactate integrals obtained from sperm incubated with $^{13}\text{C}_\text{1}$ -
438 pyruvate showed no correlation ($p > 0.05$) with concentration for either '40%' or
439 '80%' sperm populations (Figure 4c). Importantly, no correlations were found when
440 lactate peak integrals were plotted against non-sperm cell concentrations (Figures
441 4d, 4e, 4f), strongly suggesting that non-sperm cells did not make a significant
442 contribution to the metabolism observed ($p > 0.05$).

443

444 After a 4 hour incubation at 37°C , lactate peaks could be identified from all
445 substrates metabolised by '40%' and '80%' sperm ($n = 15$). The peak integral
446 measured from its MRS spectrum represents an absolute concentration of the
447 metabolite present in solution, which is a function of the sperm concentration as
448 seen in Figure 4. We reasoned vital and motile sperm would have larger impacts on
449 metabolism than immotile or dead sperm and therefore normalised lactate integrals
450 by three different methods: total sperm concentration (Figure 5a), concentration of
451 vital sperm (Figure 5b) and concentration of motile sperm (Figure 5c). Briefly, the
452 lactate integral was only significantly higher for $^{13}\text{C}_\text{u}$ -glucose incubations with '40%'
453 compared to '80%' sperm when normalised to vital concentration ($3.3 \pm 0.3 \times 10^6$ vs
454 $2.0 \pm 0.21 \times 10^6$; $p = 0.0049$) or motile concentration ($7.0 \pm 0.75 \times 10^6$ vs 4.8 ± 1.3
455 $\times 10^6$; $p = 0.0032$), Mann-Whitney test ($p < 0.0055$ taken as statistically significant).
456 No significant differences were found for these sperm populations incubated with

457 either $^{13}\text{C}_\text{u}$ -fructose or $^{13}\text{C}_\text{1}$ -pyruvate or in any incubation when normalised to total
458 sperm concentration.

459

460 After a 4 hour incubation at 37°C , bicarbonate, a marker of oxidative
461 phosphorylation, was occasionally observed. Bicarbonate was produced from $^{13}\text{C}_\text{1}$ -
462 pyruvate metabolised by '40%' sperm (5 occurrences) and '80%' sperm (3
463 occurrences), $^{13}\text{C}_\text{u}$ -glucose metabolised by '40%' sperm (2 occurrences) and '80%'
464 sperm (2 occurrences) and $^{13}\text{C}_\text{u}$ -fructose metabolised by '40%' sperm (2
465 occurrences). The appearance of bicarbonate was associated across a range of
466 sperm concentrations (mean $59.2 \times 10^6/\text{ml}$, range $17.9 - 115.4 \times 10^6/\text{ml}$) and also
467 typical non-sperm cell concentrations (mean $1.2 \times 10^6/\text{ml}$ range $0 - 2.8 \times 10^6/\text{ml}$) so
468 bicarbonate appearance was not associated with high sperm or non-sperm cell
469 concentrations. The sporadic nature of bicarbonate production and low signal to
470 noise for this peak meant that no significant differences were observed for
471 bicarbonate integrals from '40%' and '80%' sperm.

472

473 **Discussion**

474 This paper continues our previous work that used ^1H -MRS to investigate the
475 endogenous metabolites present in human sperm (Reynolds *et al.*, 2017a). Here we
476 examine human sperm metabolism of a range of exogenous ^{13}C labelled substrates
477 by ^{13}C -MRS and define the experimental conditions necessary to observe them. The
478 chosen metabolites feed into glycolysis and oxidative phosphorylation at various
479 locations in the metabolic pathways and they included sugars, ketone bodies, fatty
480 acids and amino acids. Glucose, fructose, pyruvate and lactate were chosen for their
481 role in glycolysis and their predominance in the female reproductive tract and

482 seminal fluid (Andrade-Rocha, 1999, Ford and Rees, 1990, Weed and Carrera,
483 1970), with galactose also included as its enzyme, galactose-1-phosphate
484 uridylyltransferase, has been predicted to be important for sperm motility (Asghari *et*
485 *al.*, 2017). Ketone body D-3-hydroxybutyrate was selected due to its ability to
486 maintain and restore motility of mouse sperm (Tanaka *et al.*, 2004) and the fatty acid
487 analogue butyrate was chosen as it had previously been demonstrated to be
488 metabolised by ram, bull, dog and fowl spermatozoa (Scott *et al.*, 1962). Finally,
489 amino acids glycine and glutamate feed into different aspects of oxidative
490 phosphorylation and are common amino acids found in seminal fluid which may have
491 a role in protecting sperm motility in bovine and ram spermatozoa (Kondo, 1975,
492 Setchell *et al.*, 1967, Tyler and Tanabe, 1952).

493

494 In these experiments, we found that $^{13}\text{C}_\text{U}$ -glucose and $^{13}\text{C}_\text{U}$ -fructose were
495 predominately metabolised to lactate which is indicative of glycolysis in a process
496 that also produces two net units of ATP per carbohydrate molecule. The end point of
497 glycolysis (i.e. $^{13}\text{C}_1$ -pyruvate) was also mainly converted to lactate. The enzyme
498 lactate dehydrogenase catalyzes a shuttling reaction between pyruvate and lactate
499 to maintain cofactors NADH/NAD⁺ to support further glycolysis and the electron
500 transport chain as required for cellular function.

501

502 The relative magnitude of the lactate and pyruvate ^{13}C -MRS peaks demonstrate an
503 important feature of these experiments. The degree of ^{13}C -lactate or ^{13}C -pyruvate
504 observed by ^{13}C -MRS is dependent not only on enzyme activity and substrate
505 preference but also the endogenous concentration of unlabeled lactate/pyruvate.
506 This is because any ^{13}C -lactate generated from ^{13}C -pyruvate can, in principle, be

507 converted back to ^{13}C -pyruvate. However, where there is a large concentration of
508 unlabeled ^{12}C -lactate present then there is a great probability of those molecules
509 being converted back to pyruvate, leading to ^{13}C -lactate being retained within the
510 lactate pool. Conversely, for $^{13}\text{C}_3$ -lactate sperm incubations, the lower endogenous
511 ^{12}C -pyruvate concentration resulted in fewer ^{13}C -labelled pyruvate molecules being
512 retained leading to smaller MRS pyruvate signal. Hence, how metabolites are
513 enzymatically exchanged and their endogenous concentration affects the ^{13}C MRS
514 observability of intermediate metabolites within a metabolic pathway.

515

516 In addition to pyruvate, $^{13}\text{C}_3$ -lactate often produced a small acetate peak. In
517 mammalian cells, pyruvate can be metabolised to acetyl-CoA by pyruvate
518 dehydrogenase and then to acetate by acetyl-CoA hydrolase but this will not
519 generate ATP (Knowles *et al.*, 1974). Unlike for $^{13}\text{C}_u$ -glucose and $^{13}\text{C}_u$ -fructose, ^{13}C -
520 MRS was not able to detect human sperm metabolism of $^{13}\text{C}_u$ -galactose. ^{14}C
521 galactose studies have reported that this molecule is not metabolised by human
522 sperm (MacLeod, 1941, Rogers and Perreault, 1990), however, it has been reported
523 to undergo slow glycolysis in human semen (Mann, 1946). It is likely that if galactose
524 is metabolised by human sperm then its concentration falls below the sensitivity of
525 conventional MRS.

526

527 $^{13}\text{C}_{2,4}$ -D-3-hydroxybutyrate was converted to acetoacetate catalysed by β -
528 hydroxybutyrate dehydrogenase, an enzyme that in other tissues (Smith *et al.*,
529 1969), including rat testis (Niemi and Ikonen, 1962), can be switched on by
530 environmental cues, such as starvation. The reversible conversion of
531 hydroxybutyrate to acetoacetate is linked to NADH generation and calcium uptake in

532 bovine epididymal sperm (Vijayaraghavan *et al.*, 1989) and to supporting motility in
533 mouse sperm (Tanaka *et al.*, 2004). Although acetoacetate can feed into the Krebs
534 cycle, no evidence for this was observed. Finally, there were two instances of $^{13}\text{C}_1$ -
535 butyrate conversion to glutamate. It is possible that glutamate production from $^{13}\text{C}_1$ -
536 butyrate was through Krebs cycle metabolism, however, as there were no
537 anaplerotic markers in the MRS spectrum, the exact mechanism for generation of
538 glutamate remains unknown.

539

540 Bicarbonate was occasionally produced from incubations with $^{13}\text{C}_1$ -butyrate, $^{13}\text{C}_3$ -
541 lactate, $^{13}\text{C}_{2,4}$ -D-3-hydroxybutyrate, $^{13}\text{C}_5$ -L-glutamate or $^{13}\text{C}_{1,2}$ -glycine after 24 hours,
542 but under the same conditions $^{13}\text{C}_u$ -glucose, $^{13}\text{C}_u$ -fructose or $^{13}\text{C}_1$ -pyruvate did not
543 show bicarbonate production. In aims (ii) and (iii), bicarbonate and carbon dioxide
544 production was most often observed from $^{13}\text{C}_1$ -pyruvate and, to a lesser extent, $^{13}\text{C}_u$ -
545 glucose, and least often from $^{13}\text{C}_u$ -fructose. Generally, the production of carbon
546 dioxide/bicarbonate by sperm samples was intermittent and why some samples
547 produced measurable ^{13}C -bicarbonate and others did not remains unclear as there
548 was no obvious visible bacteria, fungi, high sperm concentration or a high proportion
549 of non-sperm cells in these samples. Bicarbonate plays an important role in sperm
550 capacitation (Miraglia *et al.*, 2010) and its role in relationship to these substrates and
551 capacitation warrants further investigation.

552

553 These experiments were conducted under atmospheric oxygen and carbon dioxide
554 levels which is likely to have influenced which metabolic pathways were selected.
555 Atmospheric oxygen and carbon dioxide levels were chosen for practical reasons
556 while using the 9.4T scanner. These conditions would provide more oxygen and less

557 carbon dioxide than would be expected in vivo (Ng et al. 2018), which should
558 promote the aerobic use of OxPhos. Regardless of these conditions, OxPhos was
559 still only recorded at low levels, which does seem to suggest that human sperm
560 inherently prefer anaerobic glycolysis to meet their energy needs. This is supported
561 by Hereng et al. (2011) who also did not observe OxPhos metabolism in human
562 sperm and commented that they used glycolysis.

563

564 Rate constants for $^{13}\text{C}_\text{U}$ -glucose and $^{13}\text{C}_\text{U}$ -fructose conversion to lactate were similar,
565 suggesting that transport across the cellular membrane was not a limiting factor. The
566 estimated rate constant for $^{13}\text{C}_1$ -pyruvate to lactate was much faster than $^{13}\text{C}_\text{U}$ -
567 glucose / $^{13}\text{C}_\text{U}$ -fructose conversion to lactate. This is to be expected as the rate
568 limiting step for glycolysis is catalyzed by phosphofruktokinase which will affect
569 metabolism of both $^{13}\text{C}_\text{U}$ -glucose and $^{13}\text{C}_\text{U}$ -fructose, but not $^{13}\text{C}_1$ -pyruvate. No
570 significant differences were measured for bicarbonate rate constants estimated for
571 $^{13}\text{C}_\text{U}$ -glucose, $^{13}\text{C}_\text{U}$ -fructose or $^{13}\text{C}_1$ -pyruvate, due to large errors probably resulting
572 from the low signal to noise observed for this molecule. It was not possible to obtain
573 rates measurements for $^{13}\text{C}_3$ -lactate incubations, due to low concentrations of
574 pyruvate being produced. Whilst incubating sperm with ^{13}C labelled substrate for
575 longer would increase the magnitude of the peaks in MRS spectrum, there was a
576 concern that, over extended times, sperm death would confound the results. An
577 incubation time of 4 hours was chosen for subsequent experiments where the build-
578 up of metabolic product from the rates constant experiments in aim (ii) was
579 approximately linear.

580

581 The concentration of ^{13}C labelled substrates chosen for further experiments was 7.2
582 mM for each incubation. This is within a similar concentration range to that used by
583 Williams and Ford (2001) who found that the optimal in-vitro concentration of glucose
584 was 5.56 mM for supporting human sperm motility. $^{13}\text{C}_\alpha$ -glucose, $^{13}\text{C}_\alpha$ -fructose and
585 $^{13}\text{C}_3$ -lactate were within physiological levels experienced by sperm either within
586 seminal plasma or the female reproductive tract (Ford and Rees, 1990) (Gardner *et al.*,
587 1996). Pyruvate is found at slightly lower concentrations in seminal plasma (1 - 6
588 mM)(Mann and Lutwak-Mann, 1981) and in the female reproductive (0.1 - 0.2
589 mM)(Gardner *et al.*, 1996, Tay *et al.*, 1997). Therefore, our examinations were within
590 optimal concentration ranges to support motility for some substrates, but were super-
591 physiological for pyruvate. Our experiments used each substrate in isolation and
592 interaction between sperm and multiple substrates is likely to be different (Hereng *et al.*,
593 2011) both in vitro and in the female reproductive tract.

594

595 During preparation for assisted conception, the '40%' sperm are normally discarded
596 as they tend to be of poorer quality and also are co-localised with a higher proportion
597 of non-sperm cells (Henkel and Schill, 2003). However, these sperm are still
598 biologically relevant, as in vivo all sperm are deposited in the female reproductive
599 tract and '40%' sperm may represent a substantial fraction of the sperm population in
600 men with male factor infertility. As in our previous work using ^1H -MRS (Reynolds *et al.*,
601 2017a), we exploited the difference between these two sub-populations to test
602 the ability of ^{13}C -MRS to detect metabolism differences. First it was important to
603 consider the metabolic role of any non-sperm cells but, unlike that for sperm, the
604 concentration of non-sperm cells did not correlate with the lactate integral,
605 suggesting that they have a minimal effect on recorded lactate production at the

606 concentrations we observed for them. Therefore, the highest non-sperm cell
607 concentration in this analysis, of $6.9 \times 10^6/\text{ml}$, was taken as the limit for non-sperm
608 cell concentrations known not to affect sample metabolism measurably. Metabolism
609 of ^{13}C -labelled substrates by the differing non-sperm cells types found in seminal
610 plasma could be done in future studies.

611

612 Both '40%' and '80%' sperm produced similar amounts of ^{13}C -lactate when
613 normalised to total sperm concentration, however, unlike ^1H -MRS where sperm
614 concentration will affect metabolite detection regardless of vitality, ^{13}C -MRS will only
615 detect the ^{13}C -products of metabolising sperm. Therefore, normalising the lactate
616 signal by the vital sperm concentration was considered more appropriate.
617 Additionally, as sperm motility is estimated to account for 70% of the sperm's total
618 ATP production (Rikmenspoel, 1965), normalisation of the lactate signal by motile
619 sperm concentration was also performed. For either of these normalisations, it was
620 found that '40%' sperm incubated with $^{13}\text{C}_\text{u}$ -glucose produced more lactate, i.e. a
621 larger metabolic output, than the equivalent '80%' sperm, whereas fructose or
622 pyruvate incubations showed no significant differences between '40%' and '80%'
623 sperm.

624

625 It is interesting that only measurements after incubation with $^{13}\text{C}_\text{u}$ -glucose showed a
626 difference between motile or vital '40%' and '80%' sperm. Kinetic experiments
627 presented here suggest that $^{13}\text{C}_\text{u}$ -fructose and $^{13}\text{C}_\text{u}$ -glucose were metabolised by
628 glycolysis to similar levels and should have similar effects on sperm function. Sperm
629 are highly polarised cells and one reason for a difference between the ability of
630 glucose and fructose to support sperm motility could be related to the roles of

631 differing hexose transporter and their distribution within sperm (Angulo *et al.*, 1998,
632 Bucci *et al.*, 2011). In turn these molecules may support different phases of sperm
633 life (du Plessis *et al.*, 2015).

634

635 There are many reasons why '80%' sperm might show lower lactate production than
636 '40%' sperm. The '40%' sperm are more likely to have abnormal morphology with
637 increased cytoplasm (Aitken and West, 1990). As glycolysis is an uncontrolled
638 reaction that takes place in the cytoplasm, simply having more cytoplasm may
639 produce more lactate. Conversely, tightly controlled energy production in '80%'
640 sperm may limit ROS production and subsequent DNA damage (Aitken *et al.*, 1996).

641

642 In conclusion, we have examined sperm metabolism by ^{13}C -MRS and found
643 metabolic differences in sub-populations from the same individuals ('80%' vs. '40%'
644 sperm). Human sperm, from either sub-population, seem to predominantly use the
645 glycolytic pathway to meet their energy needs when supplied with $^{13}\text{C}_\text{u}$ -glucose or
646 $^{13}\text{C}_\text{u}$ -fructose. The level of glycolysis was increased for '40%' sperm incubated with
647 $^{13}\text{C}_\text{u}$ -glucose compared to equivalent '80%' sperm, which perhaps suggests that poor
648 quality sperm are metabolically noisy. By implication, this may also be true of poor
649 quality sperm from sub-fertile men and further work to examine this using MRS
650 technology may help to better unravel the metabolic characteristics of poor quality
651 sperm.

652

653 **Acknowledgements**

654 The authors would like to thank Dr Sarah Waite for assistance with donor recruitment
655 and appointments. We appreciate the contributions of Christopher Walls and Sophie

656 Wigfall in measuring non-sperm cell concentrations. We are also immensely grateful
657 to the Andrology Laboratory in the Jessop Wing, Sheffield, for their support with
658 recruitment and analysis.

659

660 **Authors' roles**

661 AAP, SR and MNP proposed the study. AAP and MNP obtained the MRC grant
662 funding. All authors designed the study and contributed to the writing of the
663 manuscript. SJC and SR jointly carried out experimental protocols and data analysis.
664 SJW advised on statistical analyses.

665

666 **Funding**

667 This work was funded by the MRC Grant No MR/M010473/1.

668

669 **Conflict of Interest**

670 The authors have no conflicts of interest to declare.

671

672

673

674
675
676
677
678

Figure Legends

679
680
681
682
683
684
685
686
687
688
689
690
691
692
693
694
695
696
697
698
699
700
701
702
703
704
705
706
707
708
709
710
711

Figure 1: Sperm washing methods used to remove seminal plasma. Process (A) was used to yield higher concentration of sperm for aims (i) and (ii). Process (B) was used to fractionate sperm into higher average motility, '80%', sperm and lower average motility, '40%', sperm. See main text for further details.

Figure 2: Example ^{13}C MRS spectra for sperm incubated with: (a) $^{13}\text{C}_u$ -glucose; (b) $^{13}\text{C}_u$ -fructose; or (c) $^{13}\text{C}_1$ -pyruvate. Integral locations and widths are highlighted in red. Key: sub – peaks from respective incubated substrate; L1, L2, L3 – lactate peaks, where the number indicates the carbon position, B – bicarbonate, C – carbon dioxide, U – urea.

Figure 3: Normalising the lactate integral for sperm concentration and plotting against substrate concentration showed that sperm metabolism was not limited by substrate availability as tested by Kruskal-Wallis. Sperm were tested over a 4 hour incubation ($n=3$) with $^{13}\text{C}_u$ -glucose, $^{13}\text{C}_u$ -fructose or $^{13}\text{C}_1$ -pyruvate (shown in blue, red and green respectively) at 0 mM, 1.8 mM, 3.6 mM, 7.2 mM and 14.4 mM concentrations.

Figure 4: Comparing lactate integral correlation with sperm and non-sperm cell concentrations. Sperm concentrations ($n = 15$) correlated with lactate integrals for (a) $^{13}\text{C}_u$ -glucose, (b) $^{13}\text{C}_u$ -fructose and (c) $^{13}\text{C}_1$ -pyruvate incubations. Non-sperm cell concentrations did not correlate with lactate integrals for (d) $^{13}\text{C}_u$ -glucose and (e) $^{13}\text{C}_u$ -fructose or (f) $^{13}\text{C}_1$ -pyruvate incubations. Lines of best fit are shown for correlations where $p < 0.05$ for slope being non-zero.

Figure 5: Comparing $^{13}\text{C}_u$ -glucose, $^{13}\text{C}_u$ -fructose or $^{13}\text{C}_1$ -pyruvate metabolism ($n = 15$ per substrate) between '40%' and '80%' sperm. Integrals were measured for $^{13}\text{C}_1$ -lactate and normalised against either (a) sperm concentration, (b) concentration of vital sperm or (c) concentration of motile sperm.

Legends to supplementary figures:

712
713
714
715
716
717
718
719
720
721
722
723
724
725
726
727
728
729
730
731
732
733
734
735
736
737
738
739
740
741
742
743
744
745
746
747
748
749
750
751
752
753
754
755
756
757
758
759
760

Supplementary Figure S1: Example ^{13}C -MRS spectrum of $^{13}\text{C}_3$ -lactate after a 24h incubation with sperm at 37°C . Peak assignment: S - 22.8 ppm is $^{13}\text{C}_3$ -lactate (source substrate); P - 29.2 ppm is $^{13}\text{C}_3$ -pyruvate; A - 26.0 ppm is $^{13}\text{C}_2$ -acetate; U - 165.5 ppm is ^{13}C -urea (added reference compound post incubation).

Supplementary Figure S2: Example ^{13}C -MRS spectrum of $^{13}\text{C}_{2,4}$ -D-3-hydroxybutyrate after a 24h incubation with sperm at 37°C . Peak assignment: S_2 - 49.2 ppm & S_4 - 24.5 ppm is $^{13}\text{C}_{2,4}$ -D-3-hydroxybutyrate (source substrate); B_2 - 55.9 ppm & B_4 - 32.3 ppm is $^{13}\text{C}_{2,4}$ -acetoacetate; U - 165.5 ppm is ^{13}C -urea (added reference compound post incubation).

Supplementary Figure S3: Example ^{13}C -MRS spectrum of $^{13}\text{C}_1$ -butyrate after a 24h incubation with sperm at 37°C . Peak assignment: S - 186.8 ppm is $^{13}\text{C}_1$ -butyrate (source substrate); G - 184.1 ppm is $^{13}\text{C}_5$ -glutamate; U - 165.5 ppm is ^{13}C -urea (added reference compound post incubation).

Supplementary Figure S4: Example ^{13}C -MRS spectrum of $^{13}\text{C}_{1,2}$ -glycine after a 24h incubation with sperm at 37°C . Peak assignment: S_1 - 175.1 ppm & S_2 - 44.1 ppm is $^{13}\text{C}_{1,2}$ -glycine (source substrate); U - 165.5 ppm is ^{13}C -urea (added reference compound post incubation).

Supplementary Figure S5: Example ^{13}C -MRS spectrum of $^{13}\text{C}_5$ -glutamate after a 24h incubation with sperm at 37°C . Peak assignment: S - 184.0 ppm is $^{13}\text{C}_5$ -glutamate (source substrate); U - 165.5 ppm is ^{13}C -urea (added reference compound post incubation).

Supplementary Figure S6: Example ^{13}C -MRS spectrum of $^{13}\text{C}_u$ -galactose after a 24h incubation with sperm at 37°C . Peak assignment: S between 104 - 62 ppm is $^{13}\text{C}_u$ -galactose (source substrate); U - 165.5 ppm is ^{13}C -urea (added reference compound post incubation).

Supplementary Figure S7: (a) Example ^{13}C -MRS spectrum of $^{13}\text{C}_u$ -fructose after at least 24h incubation with sperm at 37°C in the 9.4 T MRS spectrometer. Peak assignment: S is $^{13}\text{C}_u$ -fructose (source substrate between 104 - 62 ppm); L_1 - 185.3 ppm, L_2 - 71.2 ppm and L_3 - 22.8 ppm is for ^{13}C -lactate labelled in the 1, 2 or 3 position respectively; B - 162.0 ppm is bicarbonate; C - 128.0 ppm is carbon dioxide; U - 165.5 ppm is ^{13}C -urea (added reference compound). Peak integral location and range are shown as red markers. (b) Repeated spectra, acquired every 3 hours, are shown transitioning from blue to red (linearly right shifted to aid visualisation with time axis shown above a peak). Live sperm metabolism can be seen in these spectra as lactate peaks increase in size and fructose peaks decrease. (c) Integrals from $^{13}\text{C}_1$ -lactate, bicarbonate and carbon dioxide (summed over both integrals), $^{13}\text{C}_u$ -fructose and $^{13}\text{C}_3$ -lactate were repeatedly measured over time and fitted to an exponential growth curve or decay curve, as appropriate. These show how rate values were calculated from $^{13}\text{C}_u$ -fructose incubations for lactate increase and $^{13}\text{C}_u$ -fructose decline.

761 Supplementary Figure S8: (a) Example ^{13}C -MRS spectrum of $^{13}\text{C}_\text{u}$ -glucose after at
 762 least 24h incubation with sperm at 37°C in the 9.4 T MRS spectrometer. Peak
 763 assignment: S between 104 - 67.0 ppm & at 65 ppm is $^{13}\text{C}_\text{u}$ -glucose (source
 764 substrate); L_1 - 185.3 ppm, L_2 - 71.2 ppm and L_3 - 22.8 ppm is ^{13}C -lactate; B - 162.0
 765 ppm is bicarbonate; C - 128.0 ppm is carbon dioxide; U - 165.5 ppm is ^{13}C -urea
 766 (added reference compound). Peak integral location and range are shown as red
 767 markers. (b) Repeated spectra, acquired every 3 hours, are shown transitioning from
 768 blue to red (linearly right shifted to aid visualisation with time axis shown above a
 769 peak). Live sperm metabolism can be seen in these spectra as lactate peaks
 770 increase in size and glucose peaks decrease. (c) Integrals from $^{13}\text{C}_1$ -lactate,
 771 bicarbonate and carbon dioxide (summed over both integrals), $^{13}\text{C}_\text{u}$ -glucose $^{13}\text{C}_2$ -
 772 lactate and $^{13}\text{C}_3$ -lactate were repeatedly measured over time and fitted to an
 773 exponential growth curve or decay curve, as appropriate. These show how rate
 774 values were calculated from $^{13}\text{C}_\text{u}$ -glucose incubations for lactate and carbon dioxide
 775 increase and $^{13}\text{C}_\text{u}$ -glucose decline.

776
 777 Supplementary Figure S9: (a) Example ^{13}C -MRS spectrum of $^{13}\text{C}_\text{u}$ -pyruvate after at
 778 least 24h incubation with sperm at 37°C in the 9.4 T MRS spectrometer. Peak
 779 assignment: S 172.9 ppm is $^{13}\text{C}_1$ -pyruvate (source substrate); L_1 - 185.3 ppm is ^{13}C -
 780 lactate; B - 162.0 ppm is bicarbonate; C - 128.0 ppm is carbon dioxide; U - 165.5
 781 ppm is ^{13}C -urea (added reference compound) (a). Peak integral location and range
 782 are shown as red markers. (b) Repeated spectra, acquired every 3 hours, are shown
 783 transitioning from blue to red (linearly right shifted to aid visualisation with time axis
 784 shown above a peak). Live sperm metabolism can be seen in these spectra as
 785 lactate peaks increase in size and pyruvate peaks decrease. (c) Integrals from $^{13}\text{C}_1$ -
 786 lactate, bicarbonate and carbon dioxide (summed over both integrals), $^{13}\text{C}_1$ -pyruvate
 787 were repeatedly measured over time and fitted to an exponential growth curve or
 788 decay curve, if appropriate. These show how rate values were calculated from $^{13}\text{C}_1$ -
 789 pyruvate incubations for lactate and carbon dioxide increase and $^{13}\text{C}_1$ -pyruvate
 790 decline.

791
 792 Supplementary Figure S10: Example spectra of substrates incubated with sperm at
 793 different concentrations for 4 hours. (a) $^{13}\text{C}_\text{u}$ -glucose, (b) $^{13}\text{C}_\text{u}$ -fructose and (c) $^{13}\text{C}_1$ -
 794 pyruvate spectra are shown with higher concentrations of ^{13}C labelled substrate
 795 (linearly right shifted to aide visualisation, 0 mM - black spectra, 1.8 mM - orange
 796 spectra, 3.6 mM - blue spectra, 7.2 mM - green spectra and 14.4 mM - yellow
 797 spectra). The 0 mM spectra showed no substrate present or lactate created. All other
 798 concentrations produced lactate (L_1 & L_3) at similar level. However, levels of added
 799 substrate (S) depended upon the amount of substrate added and were sometimes
 800 harder to observe at the lower concentrations. ; U - 165.5 ppm is ^{13}C -urea (added
 801 reference compound). ; H - 181.1 ppm is $^{13}\text{C}_1$ -hydroxypyruvate (non-metabolically
 802 active compound in aqueous equilibrium with pyruvate)

803
 804 Supplementary Figure S11: Plotting the concentration of non-sperm cells against
 805 sperm concentration. Lines of best fit and r values are shown for correlations with $p <$
 806 0.05 for slope being non-zero, grey for '40%' sperm values and black for '80%'
 807 sperm.

808
 809

810 **References**

- 811
- 812 Aitken RJ, Buckingham DW, Carreras A, Irvine DS. Superoxide dismutase in human sperm
813 suspensions: relationship with cellular composition, oxidative stress, and sperm function.
814 *Free Radical Bio Med* 1996; **4** :495-504.
- 815 Aitken RJ, West KM. Analysis of the relationship between reactive oxygen species
816 production and leucocyte infiltration in fractions of human semen separated on Percoll
817 gradients. *Int J Androl* 1990; **6** : 433-451.
- 818 Amaral A, Paiva C, Attardo Parrinello C, Estanyol JM, Balleca JL, Ramalho-Santos J, Oliva R.
819 Identification of proteins involved in human sperm motility using high-throughput
820 differential proteomics. *J Proteome Res* 2014; **12** :5670-5684.
- 821 Andrade-Rocha FT. Seminal fructose levels in male infertility: relationship with sperm
822 characteristics. *Int Urol Nephrol* 1999; **1** :107-111.
- 823 Angulo C, Rauch MC, Droppelmann A, Reyes AM, Slebe JC, Delgado-Lopez F, Guaiquil VH,
824 Vera JC, Concha, II. Hexose transporter expression and function in mammalian spermatozoa:
825 cellular localization and transport of hexoses and vitamin C. *J Cell Biochem* 1998; **2** :189-203.
- 826 Asghari A, Marashi SA, Ansari-Pour N. A sperm-specific proteome-scale metabolic network
827 model identifies non-glycolytic genes for energy deficiency in asthenozoospermia. *Syst Biol*
828 *Reprod Med* 2017; **2** :100-112.
- 829 Barratt CLR, De Jonge CJ, Sharpe RM. 'Man Up': the importance and strategy for placing
830 male reproductive health centre stage in the political and research agenda. *Hum Reprod*
831 2018; **4** :541-545.
- 832 Bruntz RC, Lane AN, Higashi RM, Fan TW. Exploring cancer metabolism using stable isotope-
833 resolved metabolomics (SIRM). *J Biol Chem* 2017; **28** :11601-11609.
- 834 Bucci D, Rodriguez-Gil JE, Vallorani C, Spinaci M, Galeati G, Tamanini C. GLUTs and
835 mammalian sperm metabolism. *J Androl* 2011; **4** :348-355.
- 836 Buescher JM, Antoniewicz MR, Boros LG, Burgess SC, Brunengraber H, Clish CB, DeBerardinis
837 RJ, Feron O, Frezza C, Ghesquiere B et al. A roadmap for interpreting 13C metabolite
838 labeling patterns from cells. *Curr Opin Biotechnol* 2015; **34** :189-201.
- 839 du Plessis SS, Agarwal A, Mohanty G, van der Linde M. Oxidative phosphorylation versus
840 glycolysis: what fuel do spermatozoa use? *Asian J Androl* 2015; **2** :230-235.
- 841 Ford WC, Harrison A. The role of oxidative phosphorylation in the generation of ATP in
842 human spermatozoa. *J Reprod Fertil* 1981; **1** :271-278.
- 843 Ford WC, Rees JM. The bioenergetics of mammalian sperm motility. In Gagnon C (ed)
844 *Controls of Sperm Motility: Biological and Clinical Aspects*. 1990. CRC Press, Boca Raton, USA
845 pp.175-202.
- 846 Gardner DK, Lane M, Calderon I, Leeton J. Environment of the preimplantation human
847 embryo in vivo: metabolite analysis of oviduct and uterine fluids and metabolism of cumulus
848 cells. *Fertil Steril* 1996; **2** :349-353.
- 849 Henkel RR, Schill WB. Sperm preparation for ART. *Reprod Biol Endocrinol* 2003; **1** :108.
- 850 Hereng TH, Elgstoen KB, Cederkvist FH, Eide L, Jahnsen T, Skalhegg BS, Rosendal KR.
851 Exogenous pyruvate accelerates glycolysis and promotes capacitation in human
852 spermatozoa. *Hum Reprod* 2011; **12** :3249-3263.
- 853 Knowles SE, Jarrett IG, Filsell OH, Ballard FJ. Production and utilization of acetate in
854 mammals. *Biochem J* 1974; **2** :401-411.
- 855 Kondo T. Studies of free amino acids in normal and sterile human semen. *J Showa Med*
856 *Assoc* 1975; **1** :1-10.

857 MacLeod J. The metabolism of human spermatozoa. *Am J Physiol* 1941; **1** :193-201.
858 Mann T. Studies on the metabolism of semen: 3. Fructose as a normal constituent of
859 seminal plasma. Site of formation and function of fructose in semen. *Biochem J* 1946; **4**
860 :481-491.
861 Mann T, Lutwak-Mann C. *Male reproductive function and semen: themes and trends in*
862 *physiology, biochemistry and investigative andrology*. 1st edn, 1981. Springer-Verlag, Berlin,
863 Germany.
864 Miraglia E, Lussiana C, Viarisio D, Racca C, Cipriani A, Gazzano E, Bosia A, Revelli A, Ghigo D.
865 The pentose phosphate pathway plays an essential role in supporting human sperm
866 capacitation. *Fertil Steril* 2010; **7** :2437-2440.
867 Murdoch RN, White IG. Studies of the metabolism of human spermatozoa. *J Reprod Fertil*
868 1968; **3** :351-361.
869 Niemi M, Ikonen M. Cytochemistry of oxidative enzyme systems in leydig cells of rat testis
870 and their functional significance. *Endocrinology* 1962; **2** :167-174.
871 Pacey AA. Sperm, human fertility and society. In Birkhead TR, Hosken DJ and Pitnick SS (eds)
872 *Sperm biology: an evolutionary perspective*. 1st edn, 2009. Academic Press, Oxford, UK,
873 pp.565-597.
874 Peterson RN, Freund M. ATP synthesis and oxidative metabolism in human spermatozoa.
875 *Biol Reprod* 1970; **1** :47-54.
876 Reynolds S, Calvert SJ, Paley MN, Pacey AA. 1H Magnetic Resonance Spectroscopy of live
877 human sperm. *Mol Hum Reprod* 2017a; **1** :441-451.
878 Reynolds S, Ismail NFB, Calvert SJ, Pacey AA, Paley MNJ. Evidence for rapid oxidative
879 phosphorylation and lactate fermentation in motile human sperm by hyperpolarized 13C
880 Magnetic Resonance Spectroscopy. *Sci Rep* 2017b; **1** :4322.
881 Rikmenspoel R. The tail movement of bull spermatozoa: observations and model
882 calculations. *Biophys J* 1965; **4** :365-392.
883 Rogers BJ, Perreault SD. Importance of glycolysable substrates for in vitro capacitation of
884 human spermatozoa. *Biol Reprod* 1990; **6** :1064-1069.
885 Ruiz-Pesini E, Diez-Sanchez C, Lopez-Perez MJ, Enriquez JA. The role of the mitochondrion in
886 sperm function: is there a place for oxidative phosphorylation or is this a purely glycolytic
887 process? *Curr Top Dev Biol* 2007; **77** :3-19.
888 Scott TW, White IG, Annison EF. Oxidation of shortchain fatty acids (C1-C8) by ram, bull, dog
889 and fowl spermatozoa. *Biochem J* 1962; **2** :392-398.
890 Setchell BP, Hinks NT, Voglmayr JK, Scott TW. Amino acids in ram testicular fluid and semen
891 and their metabolism by spermatozoa. *Biochem J* 1967; **3** :1061-1065.
892 Shestov AA, Lee SC, Nath K, Guo L, Nelson DS, Roman JC, Leeper DB, Wasik MA, Blair IA,
893 Glickson JD. ¹³C MRS and LC-MS flux analysis of tumor intermediary metabolism. *Front Oncol*
894 2016; **6** :135.
895 Smith AL, Satterthwaite HS, Sokoloff L. Induction of brain D(-)-beta-hydroxybutyrate
896 dehydrogenase activity by fasting. *Science* 1969; **3862** :79-81.
897 Suarez SS, Pacey AA. Sperm transport in the female reproductive tract. *Hum Reprod Update*
898 2006; **1** :23-37.
899 Tanaka H, Takahashi T, Iguchi N, Kitamura K, Miyagawa Y, Tsujimura A, Matsumiya K,
900 Okuyama A, Nishimune Y. Ketone bodies could support the motility but not the acrosome
901 reaction of mouse sperm. *Int J Androl* 2004; **3** :172-177.

902 Tay JI, Rutherford AJ, Killick SR, Maguiness SD, Partridge RJ, Leese HJ. Human tubal fluid:
903 production, nutrient composition and response to adrenergic agents. *Hum Reprod* 1997; **11**
904 :2451-2456.

905 Tyler A, Tanabe TY. Motile life of bovine spermatozoa in glycine and yolkcitrate diluents at
906 high and low temperatures. *Proc Soc Exp Biol Med* 1952; **2** :367-371.

907 Vigue C, Vigue L, Huszar G. Adenosine triphosphate (ATP) concentrations and
908 ATP/adenosine diphosphate ratios in human sperm of normospermic, oligospermic, and
909 asthenospermic specimens and in their swim-up fractions: lack of correlation between ATP
910 parameters and sperm creatine kinase concentrations. *J androl* 1992; **4** :305-311.

911 Vijayaraghavan S, Bhattacharyya A, Hoskins DD. Calcium uptake by bovine epididymal
912 spermatozoa is regulated by the redox state of the mitochondrial pyridine nucleotides. *Biol*
913 *Reprod* 1989; **4** :744-751.

914 Weed JC, Carrera AE. Glucose content of cervical mucus. *Fertil Steril* 1970; **12** :866-872.

915 Williams AC, Ford WC. The role of glucose in supporting motility and capacitation in human
916 spermatozoa. *J androl* 2001; **4** :680-695.

917 Wishart DS, Feunang YD, Marcu A, Guo AC, Liang K, Vazquez-Fresno R, Sajed T, Johnson D, Li
918 C, Karu N et al. HMDB 4.0: the human metabolome database for 2018. *Nucleic acids res*
919 2018; **D1** :D608-D617.

920

921

922 Table 1: Summary of observed metabolic products of human sperm after incubating
 923 with ¹³C labelled substrates. Eight incubations were performed for each substrate at
 924 37 °C for 24h with samples subsequently stored at -80 °C prior to MRS analysis.
 925

926

Incubated substrate	Number of spectra the metabolic product was observed in		
	Lactate produced	Bicarbonate produced	Other metabolic products
¹³ C _u -glucose	8	0	-
¹³ C _u -fructose	8	0	-
¹³ C ₁ -pyruvate	8	0	-
¹³ C ₃ -lactate	N/A	2	pyruvate (7 of 8), acetate (6 of 8)
¹³ C _{2,4} -D-3-hydroxybutyrate	0	2	acetoacetate (8)
¹³ C ₁ -butyrate	0	1	glutamate (2)
¹³ C ₅ -glutamate	0	2	-
¹³ C ₂ -glycine	0	1	-
¹³ C _u -galactose	0	0	-

927

928

929 Table 2: Rate constants for ^{13}C labelled substrate consumption by human sperm (n =
 930 9 per substrate) and conversion to ^{13}C -lactate and ^{13}C -bicarbonate/ CO_2 were
 931 estimated from sequential ^{13}C MRS spectra acquired at 37°C. Peak integrals were
 932 fitted to a mono-exponential, where a negative rate constant indicates consumption
 933 of substrate. Mean \pm S.E. values shown where only fits with a Pearson correlation, r
 934 > 0.5 and significance $p < 0.01$ were retained (number of retained fits shown in
 935 parenthesis). See method for details.

937

Rate measured per peak $\times 10^5, \text{s}^{-1}$	Glucose (nf)	Fructose (nf)	Pyruvate (nf)
Incubated substrate	-1.2 ± 0.3 (8)	-0.9 ± 0.2 (9)	-10.8 ± 6.3 (7)
^{13}C -lactate	1.7 ± 0.4 (9)	1.4 ± 0.2 (9)	5.0 ± 0.8 (8)
Bicarbonate	2.4 ± 0.2 (2)	N/A	5.9 ± 0.9 (7)

938 nf: number of retained fits of 9

939

940

941 Table 3: Initial characteristics of sperm separated by DGC into two pellets '40%' and
 942 '80%' sperm (mean \pm standard deviation, except non-sperm cells which show
 943 median and range) measured. A two independent samples t-test with Welch's
 944 correction was used for data that passed a Gaussian distribution (concentration,
 945 motility and vitality) else Mann-Whitney test (non-sperm cell concentration) was used
 946 to determine differences between '40%' and '80%' sperm populations, *** $p < 0.001$,
 947 **** $p < 0.0001$.

948

949

	80% sperm (n=45)	40% sperm (n=45)	Difference
Concentration, 10^6 /ml			
Sperm	43.8 \pm 23.4	42.1 \pm 25.0	1.7
NS cell	0.4**** (0.0 – 4.5)	1.1**** (0.1 – 6.9)	0.7
Total vitality, %			
	65.0 \pm 13.8***	55.0 \pm 10.0***	10.0
Total motility, %			
	42.9 \pm 20.9***	29.5 \pm 13.8***	13.4

950

951

952 Table 4: Characteristics of '40%' and '80%' sperm populations, separated by
 953 incubated ^{13}C substrate (mean \pm standard deviation). Concentration, vitality and
 954 motility were measured the start of incubations. Differences between '40%' and
 955 '80%' sperm populations were test using a Kruskal-Wallis with Dunn's multiple
 956 comparison test. No significant differences were found.
 957

958

	$^{13}\text{C}_u$ -glucose		$^{13}\text{C}_u$ -fructose		$^{13}\text{C}_1$ -pyruvate	
	80% sperm (n=15)	40% sperm (n=15)	80% sperm (n=15)	40% sperm (n=15)	80% sperm (n=15)	40% sperm (n=15)
Concentration, $10^6/\text{ml}$						
Sperm	48.7 \pm 25.8	50.3 \pm 28.3	43.4 \pm 28.0	34.2 \pm 20.5	39.1 \pm 15.1	41.6 \pm 24.6
Total vitality, %						
0h	63.6 \pm 15.1	52.8 \pm 8.4	66.0 \pm 13.7	59.3 \pm 9.1	65.4 \pm 13.2	52.9 \pm 11.5
Total motility, %						
0h	40.9 \pm 23.1	28.0 \pm 12.7	42.3 \pm 21.2	33.4 \pm 14.4	45.5 \pm 19.5	27.3 \pm 14.2

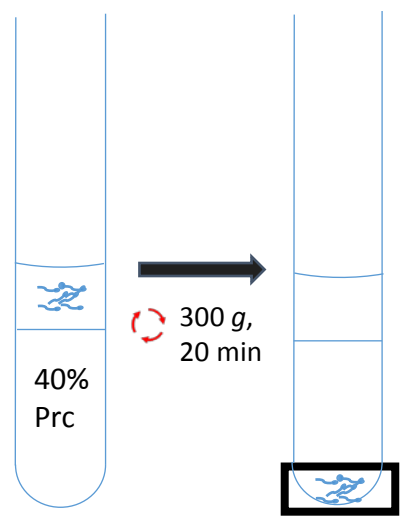
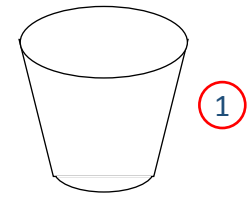
959

960

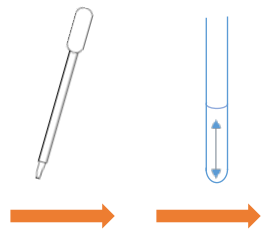
961

Semen layered onto 40% Percoll – to recover high amount of sperm

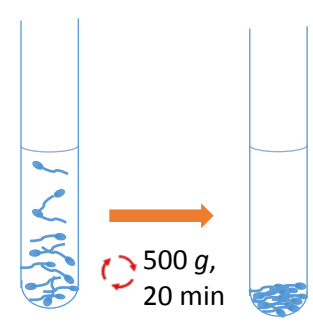
Process A



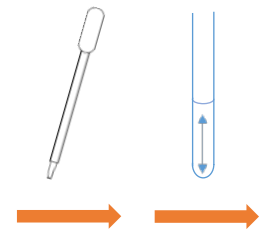
② Separate sperm from semen



③ Aspirate supernatant and collect sperm in fresh tube. Add PBS to 3 times sperm volume and resuspend

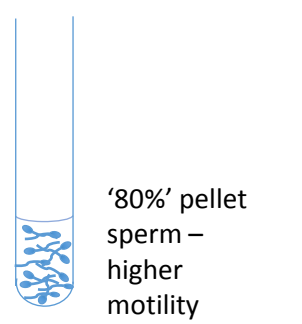
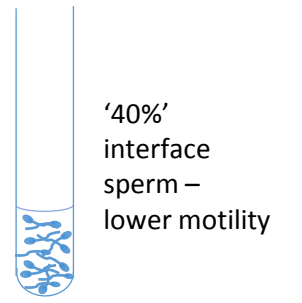
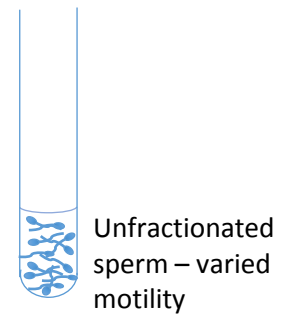


④ Separate sperm from surplus PBS and residual seminal fluid



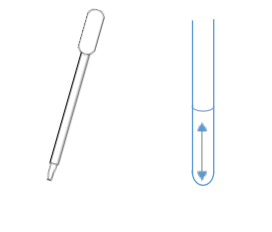
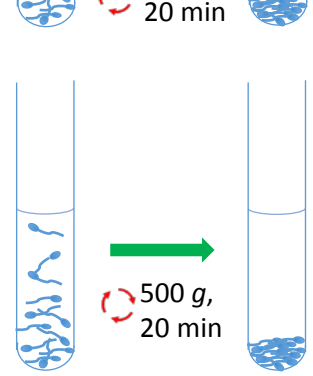
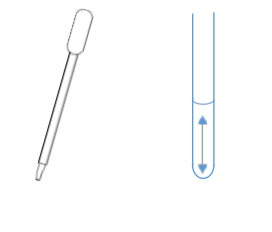
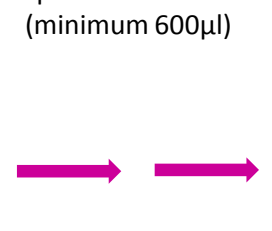
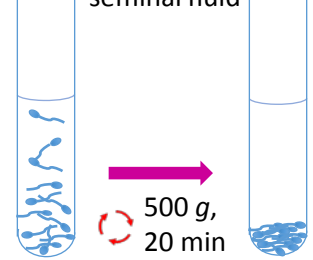
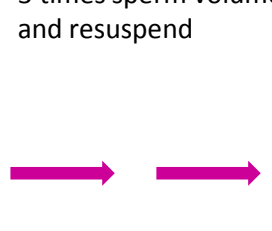
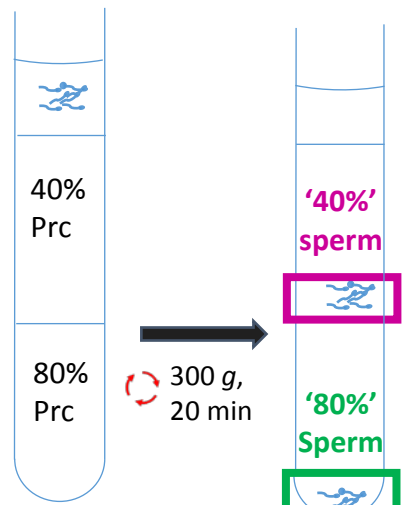
⑤ Aspirate supernatant and resuspend in fresh PBS to desired sperm concentration (minimum 600µl)

Samples used for ¹³C MRS analysis



Semen layered onto 40/80% Percoll gradients – to recover 40% and 80% sperm.

Process B



Collect sperm or aspirate supernatant

Resuspend in PBS

Centrifuge

